Spectral Change of Hadrons and Chiral Symmetry

T. Hatsuda[a]

[a]Physics Department, University of Tokyo,
Tokyo 113-0033, Japan

After a brief summary of the QCD phase structure with light quarks, we discuss two recent developments on in-medium hadrons. First topic is the σ-meson which is a fluctuation of the chiral order parameter $\bar{q}q$. Although σ is at best a broad resonance in the vacuum, it may suffer a substantial red-shift and show a characteristic spectral enhancement at the $2m_\pi$ threshold at finite temperature and baryon density. Possible experimental signatures of this phenomenon are also discussed. Another topic is the first principle lattice QCD calculation of the hadronic spectral functions using the maximum entropy method (MEM). The basic idea and a successful example of MEM are presented. Possible applications of MEM to study the in-medium hadrons in lattice QCD simulations are discussed.

1. Introduction

One of the most intriguing phenomena in quantum chromo dynamics (QCD) is the dynamical breaking of chiral symmetry. This explains the existence of the pion and dictates most of the low energy phenomena in hadron physics. The dynamical breaking of chiral symmetry is associated with the condensation of quark - anti-quark pairs in the QCD vacuum, $\langle \bar{q}q \rangle$, which is analogous to the condensation of Cooper pairs in the theory of superconductivity [1]. As the temperature (T) and/or the baryon density (n_B) increase, the QCD vacuum undergoes a phase transition to the chirally symmetric phase where $\langle \bar{q}q \rangle$ vanishes. Studying what are the possible phase structure and how the phase transition takes place are one of the main aims of the modern hadron physics [2].

When we talk about the phase structure, we need to fix appropriate variables to define the phases. Such variables in QCD are current masses of light quarks ($m_{u,d,s}$), T, and n_B. Since the following relation holds, neglecting $m_{u,d}$ in the first approximation and studying the phase structure in the m_s-T-n_B space would give us a good insight into the real world:

$$m_{u,d} \ll m_s \sim T_c \sim n_c^{1/3} \sim \Lambda_{QCD}. \tag{1}$$

Here T_c (n_c) are the critical temperature (density). In Fig.1, possible phase structures in the m_s-T plane (with n_B=0) and m_s-n_B plane (with T=0) are shown. m_s=0 (m_s=∞) corresponds to the limit of SU(3)⊗SU(3) (SU(2)⊗SU(2)) chiral symmetry. Recent lattice simulations show $T_c \simeq 175$ (155) MeV for 3 (2) flavors [3]. Furthermore, the first order transition for small m_s turns into the second order one for large m_s at the tricritical point [4]. The precise value of m_s at the tricritical point is not known yet.
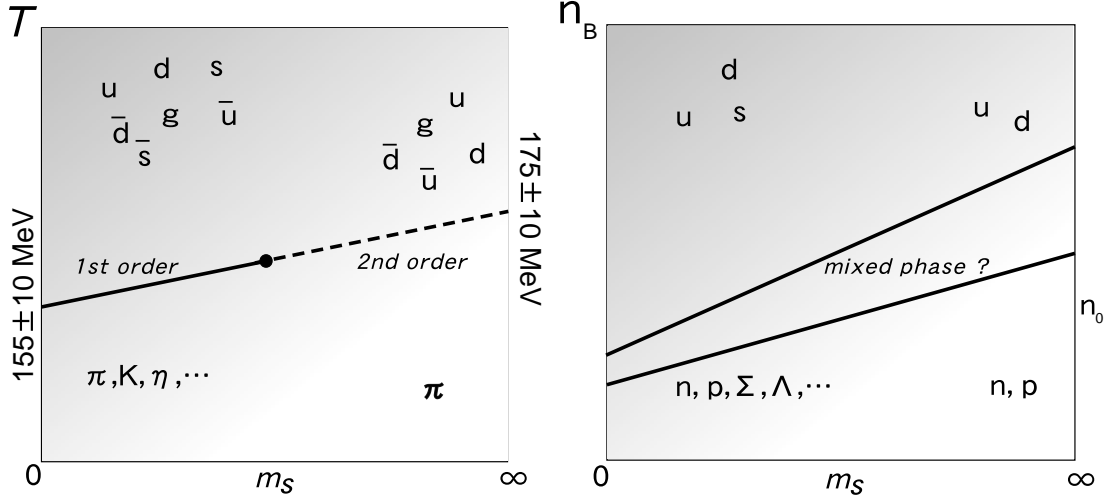
Figure 1. Possible phases in the m_s-T plane at n_B=0 (left panel) and the m_s-n_B plane at T=0. $m_{u,d}$=0 is assumed. Relevant degrees of freedom in each phase are also shown. $n_0 = 0.17\text{fm}^{-3}$ is the normal nuclear matter density.

The phase transition at finite baryon density is not well understood mostly because the information from lattice QCD is poor. Naive analysis based on the bag model shows the first order transition [5], which implies the existence of a mixed phase in the m_s-n_B plane as shown in Fig.1 (right panel). However, the possibility of a smooth hadron-quark transition is not excluded. The bag model analysis also suggests the strange quark matter as the true ground state of matter for sufficiently small m_s [6]. The system at finite baryon density, which is intrinsically quantum, is obviously richer in physics than that at finite T and has various phases such as the color superconductivity, meson condensations, and baryon superfluidity (see the reviews, [7]).

Now, what are the observables associated with the chiral transition? Model independent statement is that hadronic correlations in a same chiral multiplet (such as S (scalar)$-P^a$ (pseudo-scalar) and V_μ^a (vector)$-A_\mu^a$ (axial-vector)) should be degenerate when $\langle \bar{q}q \rangle \to 0$, namely

$$\langle S(x)S(y)\rangle \to \langle P^a(x)P^a(y)\rangle, \quad \langle A_\mu^a(x)A_\nu^b(y)\rangle \to \langle V_\mu^a(x)V_\nu^b(y)\rangle. \tag{2}$$

Thermal susceptibilities for hadronic operators $\mathcal{O}$ defined in the Euclidian space,

$$\chi_H = \int_0^{1/T} d\tau \int d^3x \langle \mathcal{O}^\dagger(\tau, \vec{x}) \mathcal{O}(0, \vec{0}) \rangle, \tag{3}$$

may be used to check such chiral degeneracy. Shown in Fig.2 is the full QCD simulation of $\sqrt{1/\chi_H}$ on the lattice with 2 light flavors [8]. One can see the degeneracy between the σ-channel (I=0, J^P=0$^+$) and the π-channel (I=1, J^P=0$^-$) above the critical point.
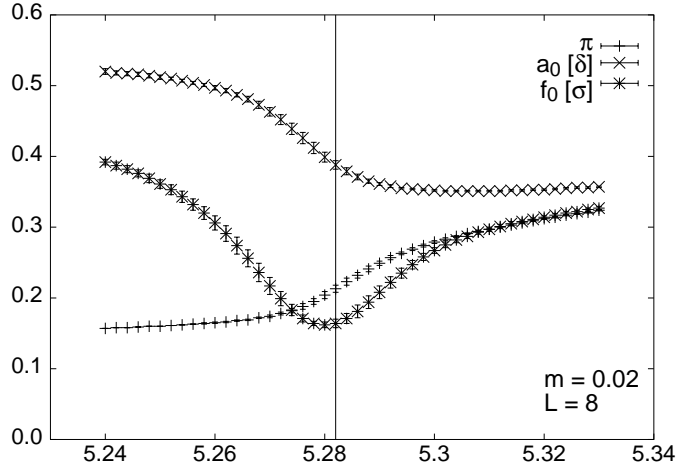
Figure 2. Thermal susceptibilities in three different channels (π, σ, and δ) for two-flavor QCD on the $8^3 \times 4$ lattice with $m_{u,d}\, a = 0.02$ [8]. The vertical (horizontal) axis denotes $\sqrt{1/\chi_H}$ (the lattice coupling $\beta = 6/g^2$).

There remains a splitting between the δ-channel ($I{=}1$, $J^P{=}0^+$) and the π-channel above the critical point, which reflects the breaking of $U_A(1)$ symmetry.

To make a direct connection with the experimental observables, however, one needs to go further and calculate the Minkowski (real-time) correlation and the hadronic spectral functions at finite T and n_B [9]. The aim of this talk is to show some recent attempts toward this goal. In Sec.2 and Sec.3, the spectral function in the σ-channel will be discussed near 2π threshold where almost model-independent argument is possible.

Experimentally, the resonances in the scalar and axial-vector channels have large width and are difficult to measure with possible exception discussed in Sec.2,3. For this reason, in-medium neutral vector-mesons which couple directly to the virtual photon have been studied both theoretically and experimentally as a probe of the chiral transition [10]. Unfortunately, theoretical calculations of the spectral function in the vector channel on the basis of the effective Lagrangians are rather model dependent, and the first principle lattice QCD study has been called for. Recently, a new promising approach was proposed: it utilizes the maximum entropy method for extracting the spectral functions from lattice QCD data. We will discuss this new development in Sec.4.

2. Spectral enhancement in hot plasma

The fluctuation of the order parameter becomes large as the system approaches to the critical point of a second order or weak first order phase transition. In QCD, the fluctuation of the phase (amplitude) of the chiral order parameter $\langle \bar{q}q \rangle$ corresponds to π (σ). The vital role of such fluctuations in the *dynamical* phenomena near the critical point at finite T was originally studied in [11,12].

It was suggested that the chiral restoration gives rise to a softening (the red-shift) of
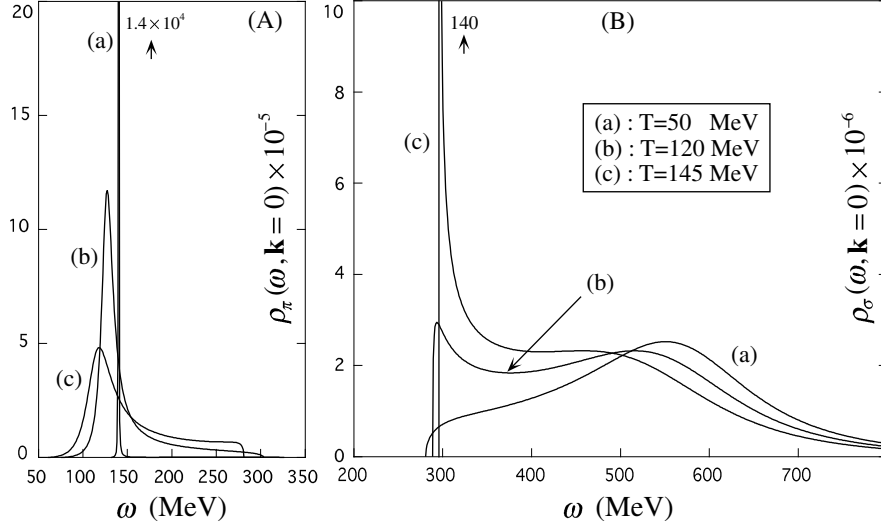
Figure 3. Spectral functions in the π channel (A) and in the σ channel (B) for T=50, 120, and 145 MeV. [15] $\rho_\sigma(\omega)$ in (B) shows only a broad bump at low T (a), while the spectral concentration is developed as T increases, (a)$\rightarrow$(b)$\rightarrow$(c).

the σ, which in turn leads to a small σ-width due to the suppression of the phase-space of the decay $\sigma \rightarrow 2\pi$ [11]. Therefore, σ may appear as a narrow resonance at finite T although it is at best a very broad resonance in the free space with a width comparable to its mass [13]. (For the phenomenological applications of this idea in relation to the relativistic heavy ion collisions, see [14].)

Further theoretical analysis by taking account the coupling $\sigma \leftrightarrow 2\pi$ shows that (i) the spectral function is the most relevant quantity for studying the true nature of σ, and (ii) the spectral function of σ has a characteristic enhancement at the 2π threshold near T_c [15]. In Fig.3, shown are the spectral functions $\rho_{\pi(\sigma)}$ in the π (σ)-channel at finite T calculated in the $O(4)$ linear σ model: Two characteristic features are the broadening of the pion peak (Fig.3(A)) and the spectral concentration at the 2π threshold ($\omega \simeq 2m_\pi$) in the σ-channel (Fig.3(B)). The latter may be measured by the 2γ spectrum from the hot plasma created in the relativistic heavy ion collisions [15].

3. Spectral enhancement in nuclear matter

$\langle \bar{q}q \rangle$ at finite baryon density obeys an exact theorem in QCD [16]:

$$\frac{\langle \bar{q}q \rangle}{\langle \bar{q}q \rangle_0} = 1 - \frac{n_B}{f_\pi^2 m_\pi^2} \left[\Sigma_{\pi N} + \hat{m} \frac{d}{d\hat{m}} \left(\frac{E(n_B)}{A} \right) \right], \tag{4}$$

where $\Sigma_{\pi N} = 45 \pm 10$ MeV is the pion-nucleon sigma term and $E(n_B)/A$ is the nuclear binding energy per particle with $\hat{m} = (m_u + m_d)/2$. $\langle \bar{q}q \rangle_0$ denotes the chiral condensate in the vacuum. The density-expansion of the right hand side of (4) gives a reduction of almost 35 % of $\langle \bar{q}q \rangle$ already at the nuclear matter density $n_0 = 0.17 \text{fm}^{-3}$.
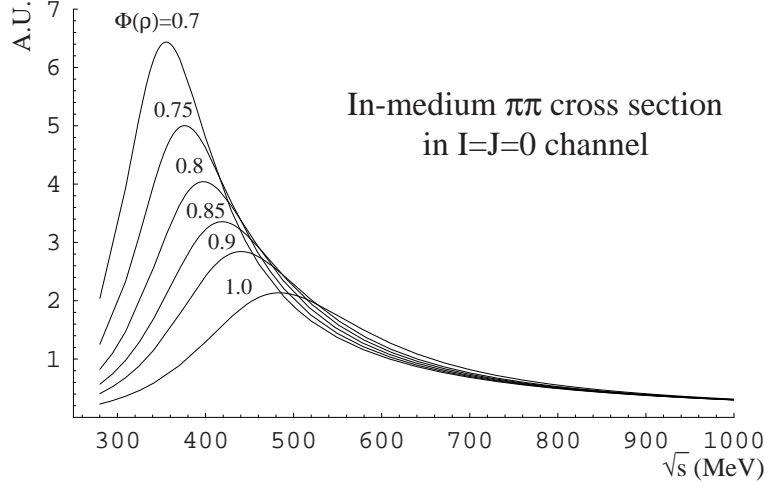
Figure 4. In-medium $\pi\pi$ cross section in the $I{=}J{=}0$ channel as a function of the c.m. energy $\sqrt{s}$ for several different values of the condensate ratio $\Phi = \langle\sigma\rangle/\langle\sigma\rangle_0$ in nuclear matter [23].

The near-threshold enhancement discussed in Sec.3 has been also studied at finite baryon density [17]. Because of the decrease of the chiral condensate discussed above, the spectral function in the σ-channel, ρ_σ, has a following generic behavior at densities not far from n_0;

$$\rho_\sigma(\omega \simeq 2m_\pi) \propto \frac{\theta(\omega - 2m_\pi)}{\sqrt{1 - \frac{4m_\pi^2}{\omega^2}}}, \qquad (5)$$

which shows a spectral concentration at the 2π threshold.

Recently CHAOS collaboration [19] reported the data on the $\pi^+\pi^\pm$ invariant mass distribution $M^A_{\pi^+\pi^\pm}$ in the reaction $A(\pi^+, \pi^+\pi^\pm)A'$ with the mass number A ranging from 2 to 208: They observed that the yield for $M^A_{\pi^+\pi^-}$ near the 2π threshold is close to zero for $A = 2$, but increases dramatically with increasing A. They identified that the $\pi^+\pi^-$ pairs in this range of $M^A_{\pi^+\pi^-}$ is in the $I{=}J{=}0$ state. This experiment was originally motivated by a possibility of strong $\pi\pi$ correlations in nuclear matter [20]. However, the state-of-the-art calculations using the nonlinear chiral Lagrangian together with $\pi N\Delta$ many-body dynamics do not reproduce the cross sections in the $I{=}0$ and $I{=}2$ channels simultaneously [21]; the final state interactions of the emitted two pions in nuclei give rise to a slight enhancement of the cross section in the $I{=}0$ channel, but is not sufficient to reproduce the experimental data. This indicates that an additional mechanism such as the partial restoration of chiral symmetry may be relevant for explaining the data [17,22].

To make a close connection between the idea of the spectral enhancement and the CHAOS data, the in-medium π-π cross section has been calculated in the linear and non-linear σ models [23]. It was shown that, in both cases, substantial enhancement of the π-π correlation in the $I{=}J{=}0$ channel near the threshold can be seen due to the partial

restoration of chiral symmetry. Furthermore, an effective 4π-N-N vertex responsible for the enhancement in the non-linear chiral Lagrangian is identified. In Fig.4, the in-medium π-π cross section in the σ-channel calculated in the O(4) linear σ model is shown.

Theoretically, it is of great importance to make an extensive analysis of the π-π interaction in heavy nuclei with the effect of partial chiral restoration to understand the CHAOS data. Experimentally, it is definitely necessary to confirm the CHAOS result not only in the same reaction but also in other reactions. Measuring $\sigma \to 2\pi^0 \to 4\gamma$ is one of the clean experiments, since it is free from the ρ meson background inherent in the $\pi^+\pi^-$ measurement. Measuring $\sigma \to 2\gamma$ is interesting because of the small final state interactions. Dilepton detection through the scalar-vector mixing in matter, $\sigma \to \gamma^* \to e^+e^-$ and the formation of the σ mesic nuclei through the nuclear reactions such as (d, t) are other possible experiments [18,17].

4. Spectral functions from lattice QCD

The lattice QCD simulations have remarkable progress in recent years for calculating the properties of hadrons as well as the properties of QCD phase transition [24]. In particular, masses of light mesons and baryons in the quenched QCD simulation agree within 5-10 % with the experimental spectra [25]. However, the lattice QCD had difficulties in accessing the dynamical quantities in the Minkowski space, because measurements on the lattice can only be carried out for discrete points in imaginary time. The analytic continuation from the imaginary time to the real time using the noisy lattice data is highly non-trivial and is even classified as an ill-posed problem.

Recently a new approach to extract spectral functions of hadrons from lattice QCD data by using the maximum entropy method (MEM) was started [26]. MEM has been successfully applied for similar problems in image reconstruction in crystallography and astrophysics, and in quantum Monte Carlo simulations in condensed matter physics [27]. There are three important aspects of MEM: (i) it does not require a priori assumptions or parametrizations of SPFs, (ii) for given data, a unique solution is obtained if it exists, and (iii) the statistical significance of the solution can be quantitatively analyzed.

4.1. Basic idea of MEM
The Euclidean correlation function $D(\tau)$ of an operator $\mathcal{O}(\tau, \vec{x})$ and its spectral decomposition at zero three-momentum read

$$D(\tau > 0) = \int \langle \mathcal{O}^\dagger(\tau, \vec{x})\mathcal{O}(0, \vec{0})\rangle d^3x \equiv \int_0^\infty K(\tau, \omega)A(\omega)d\omega, \qquad (6)$$

where ω is a real frequency, and $A(\omega)$ is the spectral function (or sometimes called the *image*), which is positive semi-definite. $K(\tau, \omega)$ is a known integral kernel (it reduces to Laplace kernel $e^{-\tau\omega}$ at zero T.)

Monte Carlo simulation provides $D(\tau_i)$ on the discrete set of temporal points $0 \leq \tau_i/a \leq N_\tau$. From this data with statistical noise, we need to reconstruct the spectral function $A(\omega)$ with continuous variable ω. This is a typical ill-posed problem, where the number of data is much smaller than the number of degrees of freedom to be reconstructed. This makes the standard likelihood analysis and its variants inapplicable unless strong assumptions on the spectral shape are made [28]. MEM is a method to circumvent this

difficulty through Bayesian statistical inference of the most probable *image* together with its reliability.

Let's start with the Bayes' theorem: $P[X|Y] = P[Y|X]P[X]/P[Y]$, where $P[X|Y]$ is the conditional probability of X given Y. The most probable image $A(\omega)$ for given lattice data D is obtained by maximizing the conditional probability

$$P[A|D] \propto P[D|A]P[A]. \tag{7}$$

The reliability of the obtained result can be checked by the second variation of $P[A|D]$ with respect to $A(\omega)$.

$P[D|A]$ in (7) is a standard χ^2, namely $P[D|AH] = Z_L^{-1} \exp(-L)$ with a likelihood function $L = (1/2) \sum_{i,j} (D(\tau_i) - D^A(\tau_i)) \, C_{ij}^{-1} \, (D(\tau_j) - D^A(\tau_j))$ and a normalization factor Z_L. $D(\tau_i)$ is the lattice data averaged over gauge configurations and $D^A(\tau_i)$ is the correlation function obtained by given A. C is a covariance matrix of the data.

$P[D|A]$ (the prior probability) in (7), can be written with parameters α and m as $P[A] = Z_S^{-1} \exp(\alpha S)$ by the combinatorial argument. Here S is the generalized information entropy,

$$S = \int_0^\infty \left[A(\omega) - m(\omega) - A(\omega) \log \left(\frac{A(\omega)}{m(\omega)} \right) \right] d\omega, \tag{8}$$

with Z_S being a normalization factor. α is a real and positive parameter and $m(\omega)$ is a real and positive function called the default model.

The output image A_{out} is given by a weighted average over A and α:

$$A_{out}(\omega) = \int A_\alpha(\omega) \, P[\alpha|Dm] \, d\alpha, \tag{9}$$

where $A_\alpha(\omega)$ is obtained by minimizing the "free-energy" $F \equiv L - \alpha S$. α dictates the relative weight of the entropy S (which tends to fit A to the default model m) and the likelihood function L (which tends to fit A to the lattice data). Note that α appears only in the intermediate step and is integrated out in the final result.

One can prove that the solution of $\delta F = 0$ is unique if it exits. The error analysis of the reconstructed image can be studied by evaluating the second derivative of the free energy $\delta^2 F/\delta A(\omega)\delta A(\omega')$. The default model m is chosen such that the error becomes minimum.

4.2. MEM with lattice data

In Fig.5, shown is an example of the spectral function in the pion and the rho meson channels at $T = 0$ extracted from the quenched lattice QCD data [26]. The lattice size is $20^3 \times 24$ with $\beta = 6.0$, which corresponds to $a = 0.0847$ fm ($a^{-1} = 2.33$ GeV), and the spatial size of the lattice $L_s a = 1.69$ fm. Hopping parameters are chosen to be $\kappa = 0.153$, 0.1545, and 0.1557 with $N_{conf} = 161$ for each κ. For the quark propagator, the Dirichlet (periodic) boundary condition is employed for the temporal (spatial) direction. We use data at $1 \leq \tau_i/a \leq 12$.

The obtained images have the low-energy peaks corresponding to π and ρ, and the broad structure in the high-energy region. The mass of the ρ-meson in the chiral limit extracted from the peak in Fig.5 is consistent with that determined by the asymptotic behavior of $D(\tau)$. Although the maximum value of the fitting range $\tau_{max}/a = 12$ marginally covers
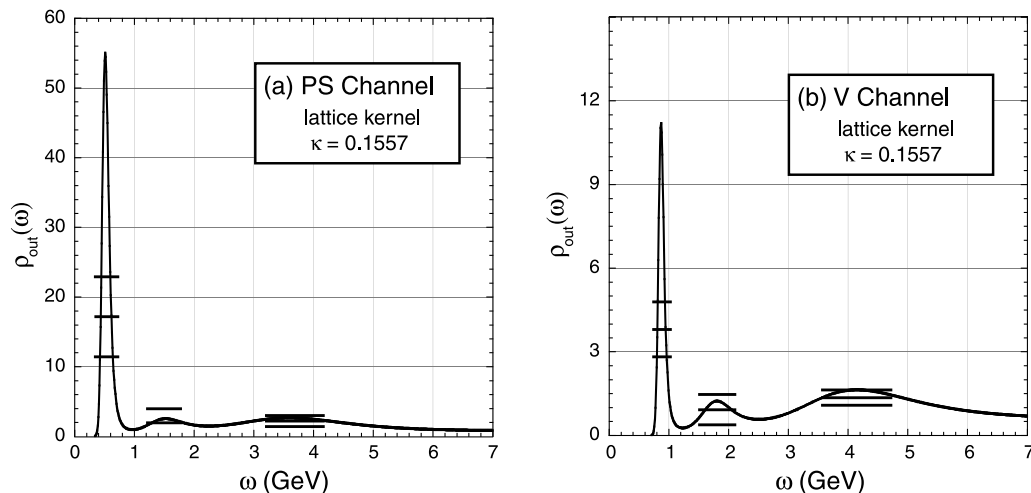
Figure 5. Spectral functions $\rho_{out}(\omega) \equiv A_{out}(\omega)/\omega^2$ obtained by MEM using the quenched lattice QCD data. The lattice size is $20^3 \times 24$ with $a = 0.0847$ fm. 12 data points in the temporal direction ($1 \leq \tau_i/a \leq 12$) are used for the MEM analysis. (a) is for the pion channel and (b) is for the rho-meson channel. The figures are taken from [26].

the asymptotic limit in τ, we can extract reasonable masses for π and ρ. The width of π and ρ in Fig.5 is an artifact due to the statistical errors of the lattice data. In fact, in the quenched approximation, there is no room for the ρ-meson to decay into two pions.

As for the second peaks, the error analysis shows that their spectral "shape" does not have much statistical significance, although the existence of the non-vanishing spectral strength is significant. Under this reservation, we fit the position of the second peaks and made linear extrapolation to the chiral limit and obtain results consistent with experimental data on π' and ρ'.

The error in Fig.5 indicates the uncertainty of the spectrum averaged over the interval in the frequency space. Better data with smaller a and larger lattice volume will be helpful for obtaining spectral functions with smaller errors.

4.3. The future of MEM

MEM introduces a new way of extracting physical information from the lattice QCD data. It is now time to study how hadrons are modified in the medium using this new approach. The long-standing problem of in-medium spectral functions of vector mesons (ρ, ω, ϕ, J/ψ, Υ, $\cdots$, etc) and scalar/pseudo-scalar mesons (σ, π, $\cdots$, etc) can be studied using MEM combined with finite T lattice simulations. The in-medium behavior of the light vector mesons [29] and scalar mesons [11] is intimately related to the chiral restoration in hot/dense matter, while that of the heavy vector mesons is related to deconfinement [30]. Simulations with an anisotropic lattice is necessary for this purpose to have enough data points in the temporal direction at finite T, which is now under way [31]. (See also an attempt on the basis of NRQCD simulation [32].) It is interesting to study the spectral

functions with finite three-momentum **k** for treating moving-hadrons in the medium.

Non-perturbative collective modes above the critical temperature of the QCD phase transition speculated in [11,33,34] may be studied efficiently by using MEM, since the method does not require any specific ansätze for the spectral shape. Correlations in the diquark channels in the vacuum and in medium are interesting to be explored in relation to the q-q correlation in baryon spectroscopy and to color superconductivity at high n_B [35].

5. Summary

Although the light σ-meson does not show up clearly in the free space because of its large width due to the strong coupling with two pions, it may appear as a soft and narrow collective mode in the hadronic medium when the chiral symmetry is (partially) restored. A characteristic signal is the enhancement of the spectral function and the π-π cross section near the 2π threshold. They could be observed in the hadronic reactions with heavy nuclear targets as well as in the heavy ion collisions through the detection of pion pairs and photon pairs. Finding such signal provides us with a better understanding of the non-perturbative structure of the QCD vacuum and its quantum fluctuations.

The maximum entropy method (MEM) opens the door to extract the spectral functions from the first principle lattice QCD data without making a priori assumptions on the spectral shape. The method has been tested at T=0 with reasonable success. The uniqueness of the solution and the quantitative error analysis make MEM superior to any other approaches adopted previously. The method has a promising future for analyzing in-medium properties of hadrons and its relation to chiral structure of matter.

REFERENCES

1. Y. Nambu, Nucl. Phys. **A638** (1998) 35c.
2. T. Hatsuda and T. Kunihiro, Phys. Rep. **247** (1994) 221.
3. F. Karsch, hep-ph/0103314, these proceedings.
4. R. D. Pisarski and F. Wilczek, Phys. Rev. **D29** (1984) 338. F. Wilczek, Int. J. Mod. Phys. **A7** (1992) 3911, 6951; Int. J. Mod. Phys. **D3** (1994) 63.
5. H. Heiselberg and M. Hjorth-Jensen, Phys. Rep. **328** (2000) 237.
6. J. Madsen, astro-ph/9809032.
7. K. Rajagopal and F. Wilczek, hep-ph/0011333.
   Brown and Rho, hep-ph/0103102 (to appear in Phys. Rep).
8. F. Karsch, Nucl. Phys. B (Proc. Suppl.) **83** (2000) 14.
9. See the review, E. V. Shuryak, Rev. Mod. Phys. **65** (1993) 1.
10. See the reviews, R. Rapp and J. Wambach, Adv. Nucl. Phys. **25** (2000) 1.
    J. Alam, S. Sarkar, P. Roy, T. Hatsuda and B. Sinha, Ann. Phys. (N.Y.), **286** (2000) 159. G. Chanfray, nucl-th/0012068.
11. T. Hatsuda and T. Kunihiro, Phys. Rev. Lett. **55** (1985) 158; Phys. Lett. **B185** (1987) 304.
12. K. Rajagopal and F. Wilczek, Nucl. Phys. **B399** (1993) 395 .
13. D.E. Groom et al. (Particle Data Group), Eur. Phys. J. **C15** (2000) 1.
    Proceedings of "Possible Existence of the σ-Meson and its Implications to Hadron

Physics", KEK-Proceedings/2000-4, (Proc. site,
http://amaterasu.kek.jp/YITPws/online/index.html).

14. H. A. Weldon, Phys. Lett. **B274** (1992) 133. C. Song and V. Koch, Phys. Lett. **B404** (1997) 1. M. Stephanov, K. Rajagopal and E. Shuryak, Phys. Rev. Lett. **81** (1998) 4816. J. Schaffner-Bielich, Phys. Rev. Lett. **84** (2000) 3261.

15. S. Chiku and T. Hatsuda, Phys. Rev. **D57** (1998) R6, ibid. **D58** (1998) 076001. M. K. Volkov et al., Phys. Lett. **B424** (1998) 235.

16. E. G. Drukarev and E. M. Levin, Prog. Paet. Nucl. Phys. **A556** (1991) 467. R. Brockmann and W. Weise, Phys. Lett. **B367** (1996) 40.

17. T. Hatsuda, T. Kunihiro and H. Shimizu, Phys. Rev. Lett. **82** (1999) 2840.

18. T. Kunihiro, Prog. Theor. Phys. Supplement **120** (1995) 75.

19. F. Bonutti *et al.* (CHAOS Collaboration), Nucl. Phys. **A677** (2000) 123.

20. See e.g., G. Chanfray, Z. Aouissat, P. Schuck and W. Nörenberg, Phys. Lett. **B256** (1991) 325.

21. R. Rapp *et al.*, Phys. Rev. **C59** (1999) R1237. M. J. Vicente-Vacas and E. Oset, Phys. Rev. **C60** (1999) 064621.

22. Z. Aouissat, G. Chanfray, P. Schuck and J. Wambach, Phys. Rev. **C61**, 012202 (2000). D. Davesne, Y. J. Zhang and G. Chanfray, Phys. Rev. **C62** (2000) 024604 .

23. D. Jido, T. Hatsuda and T. Kunihiro, Phys. Rev. **D63** (2001) 011901.

24. Lattice 2000 Proceedings, Nucl. Phys. B (Proc. Suppl.) **94** (2000) 1.

25. S. Aoki et al., Phys. Rev. Lett. **84** (2000) 238.

26. Y. Nakahara, M. Asakawa and T. Hatsuda, Phys. Rev. **D60** (Rapid Comm.) (1999) 091503; Nucl. Phys. B (Proc. Suppl.) **83** (2000) 191; hep-lat/0011040 to appear in Prog. Part. Nucl. Phys. **47** (2001).
    For earlier attempts to aim a similar goal, Ph. de Forcrand et al., Nucl. Phys. B (Proc. Suppl.) **63A-C** (1998) 460; E. G. Klepfish, C. E. Creffield and E. P. Pike, Nucl. Phys. B (Proc. Suppl.) **63A-C** (1998) 655.

27. B. R. Frieden, J. Opt. Soc. Am., **62** (1972) 511. M. Jarrell and J. E. Gubernatis, Phys. Rep. **269** (1996) 133. N. Wu, *The Maximum Entropy Method*, (Springer-Verlag, Berlin, 1997).

28. T. Hashimoto, A. Nakamura and I. O. Stamatescu, Nucl. Phys. **B400** (1993) 267; ibid. **B406** (1993) 325. M. -C. Chu, J. M. Grandy, S. Huang and J. W. Negele, Phys. Rev. D **48** (1993) 3340. D. B. Leinweber, Phys. Rev. D **51** (1995) 6369. D. Makovoz and G. A. Miller, Nucl. Phys. **B468** (1996) 293. C. Allton and S. Capitani, Nucl. Phys. **B526** (1998) 463. Ph. de Forcrand et al. (QCD-TARO Collaboration), hep-lat/0008005.

29. R. D. Pisarski, Phys. Lett. **B110** (1982) 155. G. E. Brown and M. Rho, Phys. Rev. Lett. **66** (1991) 2720. T. Hatsuda and S. Lee, Phys. Rev. **C46** (1992) R34.

30. T. Hashimoto et al., Phys. Rev. Lett. **57** (1986) 2123. T. Matsui and H. Satz, Phys. Lett. **B178** (1986) 416.

31. M. Asakawa and T. Hatsuda, in progress.

32. M. Oevers, C. Davies and J. Shigemitsu, Nucl. Phys. B (Proc. Suppl.) **94** (2001) 363.

33. C. DeTar, Phys. Rev. **D32** (1985) 276.

34. A. Peshier and M. Thoma, Phys. Rev. Lett. **84** (2000) 841. F. Karsch, M. G. Mustafa and M. H. Thoma, Phys. Lett. **B 497** (2001) 249.

35. I. Wetzorke and F. Karsch, hep-lat/0008008.